**JOURNAL OF THEORETICAL AND APPLIED MECHANICS**
**45**, 2, pp. 363-377, Warsaw 2007

# THEORETICAL AND EXPERIMENTAL STUDIES OF ENERGY DISSIPATION IN A MODEL OF A RING SPRING

Zbigniew Skup

*Institute of Machine Design Fundamentals, Warsaw University of Technology*
*e-mail: zskup@ipbm.simr.pw.edu.pl*

The paper presents the problem of energy dissipation in ring spring joints with structural friction taken into account. A comparative analysis has been conducted to compare theoretical results obtained by means of numerical simulation with results of experimental research assisted by an MTS testing machine. This contribution shows an outline of theoretical considerations, the method of experimental tests as well as selected comparative results.

*Key words:* ring spring, energy dissipation, structural friction, hysteretic loop, experimental testing

## 1. Introduction

The subject of analytical considerations is a friction pair consisting of cooperating conical-shaped friction surfaces of internal and external rings of a ring spring. That type of a spring is applied in ring buffers and friction dampers used to dissipate energy. Contact deformation, friction and damping of vibrations occurring in temporary fastenings and permanent joints have essential influence on dynamical properties of machines and devices. Mathematical description of structural friction phenomena is not easy due to complexity of the friction process and difficulties in describing the state of stresses and deformations occurring in joints of elements. Therefore, the description is based on simplifying assumptions and fundamental mechanical laws that apply to patterns of stress and deformations arising during tension, torsion, compression, shearing (see References).

The following assumptions are made in order to analyze the ring spring: the distribution of unit pressure between cooperating surfaces of the contact joint is uniform; there is a constant friction coefficient of contacting elements for an arbitrary value of the unit pressure; the friction force is subject to the

Coulomb Law; and, consequently, the frictional resistance is proportional to pressure, while material properties are described by the Hooke Law; friction is fully developed in the sliding zone; inertia forces are neutral (due to very low acceleration values); and flat sections are assumed (cross-sections remained flat after the deformation of elements). Apart from a theoretical study of the model shown in Fig. 2, experimental tests have been conducted on a real system (Fig. 1).

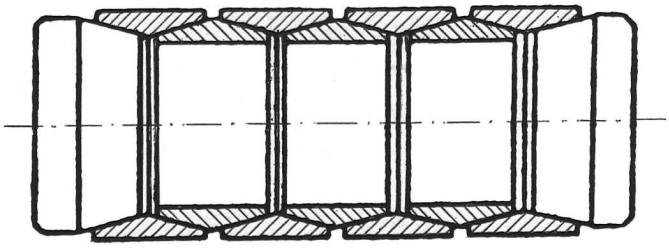

Fig. 1. A simplified model of a real ring spring

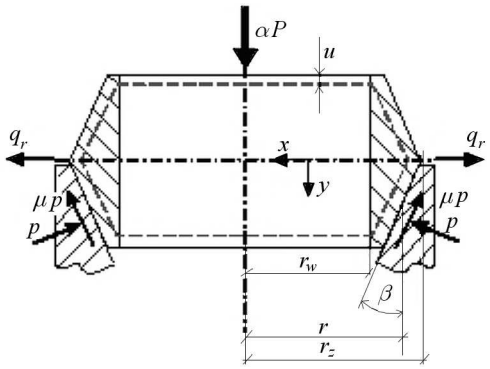


Fig. 2. A simplified model of the contact joint of the friction pair in the ring spring

## 2. Determination of displacements in particular stages during loading the friction pair

Analytical investigations have been conducted on a ring spring model with pure friction interaction between the elements. It is the closest approximation of the results obtained from experiments. The simplifications taken in the paper are a result of assumptions related to the theory of axially-symmetrical thin-walled rings. Thus, a simplified model was assumed for analytical investigations – a model of contact consisting of external and internal rings loaded

with an axial force $\alpha P$, as presented in Fig. 2, where: $r$ is the average radius of the conical surface of the internal ring, $r_z$, $r_w$ – external and internal radii of the conical surface of the ring, $\beta$ – angle of tilt of the conical surface of the ring.

**Stage 1 – Loading the system with the axial force** $\alpha P$ $(0 \leqslant \alpha \leqslant \alpha_1 = 1)$

By projecting the forces in the axial direction, we obtain the following relationship

$$2\pi r(p\sin\beta + \mu p\cos\beta) = \alpha P \tag{2.1}$$

while projection in the radial direction yields

$$2(p\cos\beta - \mu p\sin\beta) = q_r \tag{2.2}$$

where: $p$ denotes the unit pressure per unit length, $\mu$ – friction coefficient, $\alpha P$ – axial load of the system $(0 \leqslant \alpha \leqslant 1)$, $q_r$ – radial load per unit length.

Having determined the unit pressure $p$ from equation (2.1), and substituted it to equation (2.2), we obtain

$$q_r = \frac{\alpha P}{\pi r}\Big(\frac{\cos\beta - \mu\sin\beta}{\sin\beta + \mu\cos\beta}\Big) = \frac{\alpha P}{\pi r}\Big(\frac{1 - \mu\tan\beta}{\mu + \tan\beta}\Big) \tag{2.3}$$

In accordance with the Hooke Law, given a uni-axial stress, the strain $\varepsilon$ can be described with the following dependence

$$\varepsilon = \frac{N}{EF} = \frac{rq_r}{EF} \tag{2.4}$$

where: $E$ is Youngs elasticity modulus, $F$ – cross-sectional area of the ring.

Due to deformation of the two co-operating rings, the axial displacement can be determined from

$$u = 2\Delta r\cot\beta = 2\varepsilon r\cot\beta \tag{2.5}$$

The dependence between the displacement $u$ of the ring and its external load $\alpha P$ can be determined by substituting (2.3) and (2.4) to formula (2.5). Therefore, after transformations, we can obtain the following

$$u = \frac{2\alpha Pr}{\pi EF}\Big(\frac{\cot\beta - \mu}{\tan\beta + \mu}\Big) \tag{2.6}$$

Equation (2.6) shows interval 1 of the straight line $OA_1$ in Fig. 3. The maximum displacement $u_{max}$ for the final stage of loading with $\alpha = 1$ can be described with the following formula

$$u_{max} = \frac{2Pr}{\pi EF}\Big(\frac{\cot\beta - \mu}{\tan\beta + \mu}\Big) \tag{2.7}$$

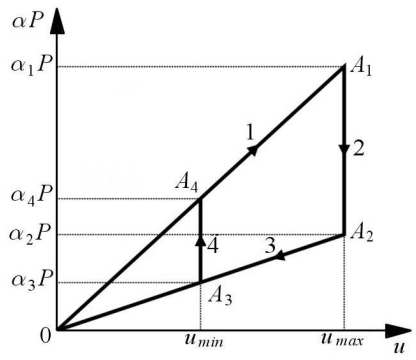


Fig. 3. Hysteretic loop for the friction pair of the ring spring

**Stage 2 – Unloading of the system without sliding** $(\alpha_2 \leqslant \alpha \leqslant \alpha_1)$

The unloading decreases from the force value $P$ down to $\alpha_2 P$ (interval 2 of the straight line $A_1A_2$ – Fig. 3), and it does not produce any changes in the displacement $u_{max}$. Therefore, the cooperating surfaces do not slide.

**Stage 3 – Unloading of the system with sliding** $(\alpha_3 \leqslant \alpha \leqslant \alpha_2)$

When sliding occurs between the cooperating surfaces, this phenomenon is accompanied by the change of sense of the friction forces. Therefore, equations of equilibrium of forces projected on the axis of symmetry and radial direction are the following

$$\begin{aligned} 2\pi r(p\sin\beta - \mu p\cos\beta) &= \alpha P \\ 2(p\cos\beta - \mu p\sin\beta) &= q_r \end{aligned} \tag{2.8}$$

Having determined the unit pressure from equation (2.8) and substituted it to equation (2.9), we obtain

$$q_r = \frac{\alpha_2 P}{\pi r}\Big(\frac{1+\mu\tan\beta}{\tan\beta - \mu}\Big) \tag{2.9}$$

To make the ring spring perform in the right way, i.e. so that the considered system would not lock itself, equation (2.10) has a physical sense when $\tan\beta > \mu$ – then the system will not be a self-locking one.

Following the steps taken at the first stage of loading, and applying formula (2.6) while taking account of (2.10), we obtain a relation between the axial displacement of the rings and their loading

$$u = \frac{2\alpha_2 Pr}{\pi EF}\Big(\frac{\cot\beta + \mu}{\tan\beta - \mu}\Big) \tag{2.10}$$

From the equality of displacements for loading, see formula (2.7), and unloading, see (2.11), we find the parameter $\alpha_2$

$$\alpha_2 = \frac{(\cot\beta - \mu)(\tan\beta - \mu)}{(\tan\beta + \mu)(\cot\beta + \mu)} \tag{2.11}$$

The minimum displacement can be determined from formula (2.11) with $\alpha_2 = \alpha_3$, that is

$$u_{min} = \frac{2\alpha_3 Pr}{\pi EF}\Big(\frac{\cot\beta + \mu}{\tan\beta - \mu}\Big) \tag{2.12}$$

The displacement $u_{min}$ corresponds to interval 4 of the straight line $A_3A_4$ of the hysteretic loop (Fig. 3).

**Stage 4 – Repeated increase of loading in the system without sliding** $(\alpha_4 \leqslant \alpha \leqslant \alpha_3)$

At this stage, when the loading is increased again from $\alpha_3 P$ to $\alpha_4 P$, the displacement does not change. The parameter $\alpha_4$ can be determined as shown above from the comparison of the same displacements defined by (2.6) and (2.13); thus

$$\alpha_4 = \alpha_3 \frac{(\cot\beta + \mu)(\tan\beta + \mu)}{(\tan\beta - \mu)(\cot\beta - \mu)} = \frac{\alpha_3}{\alpha_2} \tag{2.13}$$

## 3. Determination of energy dissipated during one cycle of loading

The dissipated energy in one cycle of loading equals is (Fig. 3)

$$\psi = \Big(\frac{\alpha_4 P - \alpha_3 P + P - \alpha_2 P}{2}\Big)(u_{max} - u_{min}) \tag{3.1}$$

Having used relationships (2.7), (2.11), (2.12) and (2.13), we obtained

$$\psi = \frac{P^2 r}{\pi EF}\Big[\frac{d}{a}\Big(1 - \frac{bd}{ac}\Big) + \frac{c\alpha_3^2}{b}\Big(1 - \frac{ac}{bd}\Big)\Big] \tag{3.2}$$

where

$$\begin{aligned} &a = \tan\beta + \mu \qquad && b = \tan\beta - \mu \qquad && c = \cot\beta + \mu \\ &d = \cot\beta - \mu \qquad && \tan\beta > \mu \end{aligned} \tag{3.3}$$

Formula (3.2) has a physical sense in the case of $\tan\beta > \mu$ – the rings would not jam then.

## 4. Results of simulation testing

The simulation testing was conducted with the use of Mathematica 4.1 program. Numerical calculations were carried out with the use of computer programs written in C language. These applications allowed for modifications of the following: medium radius of cooperating surfaces of the friction pair consisting of external and internal rings, friction coefficient, angle of tilt of cooperating conical surfaces of the rings, Young's modulus and the stress range of rings of the spring (through the change of the parameters $\alpha_1$ and $\alpha_3$), which made it possible to conduct a precise analysis of the joint. The numerical calculations were made for the experimental model tested that had the following parameters: $F = 132.94\,\mathrm{mm}^2$, $E = 2.1 \cdot 10^5\,\mathrm{N/mm}^2$, $r = 37.25\,\mathrm{mm}$, $\beta = 12^\circ$, $P = 28\,\mathrm{kN}$, $\mu = 0.15$.

Table 1 shows a comparison of energy losses (the area of hysteretic loops) obtained as a result of computational simulations.

**Table 1.** Energy losses obtained from computational simulations for different loadings

| No. of diagram | $P$ [kN] | $u_{max}$ [m] | $\psi$ [Nm] |
|---|---|---|---|
| 1 | 15 | 0.000160066 | 0.000622207 |
| 4 | 20 | 0.000213422 | 0.001106150 |
| 3 | 25 | 0.000266777 | 0.001728350 |
| 4 | 28 | 0.000298791 | 0.002168040 |

The results of numerical calculations are shown in Fig. 4-Fig. 12. Interesting processes of energy losses in function of the ring average radius and in function of the loading for different angles of tilt of the conical surface are show in Fig. 5 and Fig. 6. Energy losses in function of the loading for different values of the average radius are nonlinear (Fig. 7).

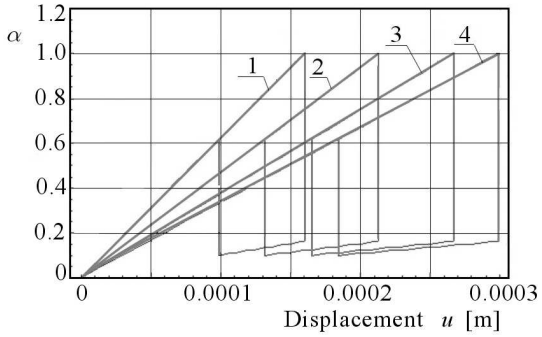


Fig. 4. Hysteretic loops for different loadings $P$: 1 – 15 kN, 2 – 20 kN, 3 – 25 kN, 4 – 28 kN

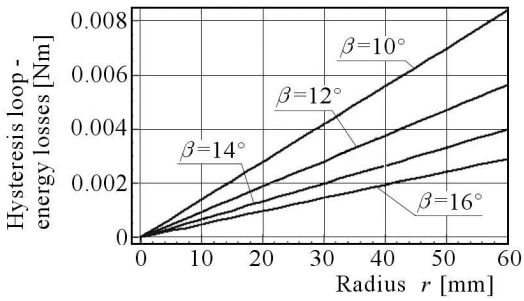


Fig. 5. Energy losses in function of the average radius for different coning angles ($\mu = 0.15$)

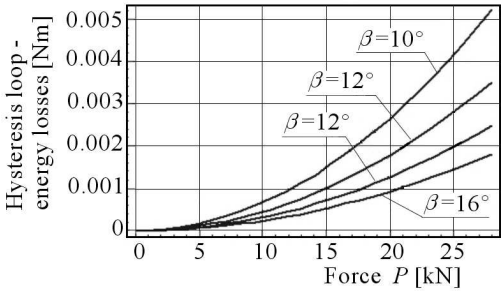


Fig. 6. Energy losses in function of the loading for different coning angles ($\mu = 0.15$, $r = 37.25\,\mathrm{mm}$)

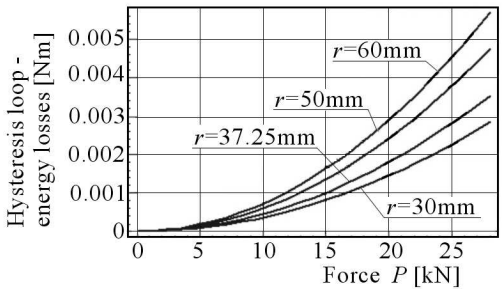


Fig. 7. Energy losses in function of the loading for different average radii ($\mu = 0.15$, $\beta = 12°$)

The diagrams indicate that energy losses increase as the coning angle decreases. Figure 8 shows that in the case of complete unloading and given the range of the coefficient of friction $\mu = 0.14$-$0.22$, the energy losses are optimal. When the system is unloaded by 5-20%, the energy losses are optimal for the coefficient of friction $\mu = 0.21$ (Fig. 9). The axial displacement of rings in function of the coning angle or in function of the coefficient of friction is nonlinear (Fig. 10 and Fig. 11). Figure 12 demonstrates that the axial displacement of

the rings under the influence of loading and changes in the average radius of the rings is linear.

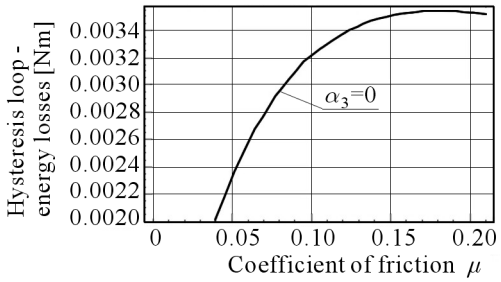


Fig. 8. Energy losses in function of the coefficient of friction for completely unloaded system $(\beta = 12°)$

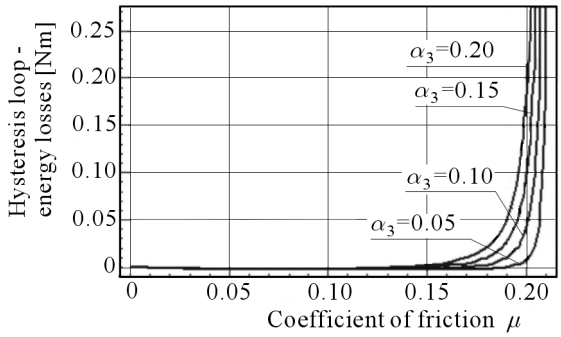


Fig. 9. Energy losses in function of the coefficient of friction for different degrees of unloading $(\beta = 12°)$

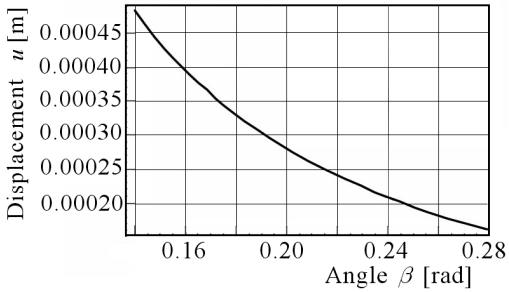


Fig. 10. The displacement $u$ in function of the coning angle for $\mu = 0.15$

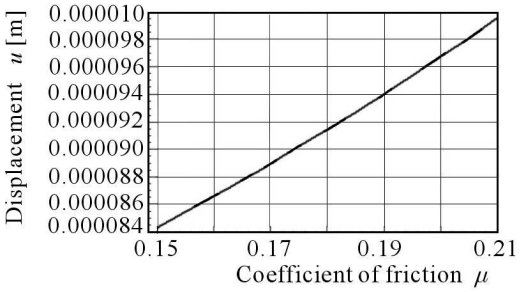


Fig. 11. The displacement $u$ in function of the coefficient of friction ($\beta = 12°$)

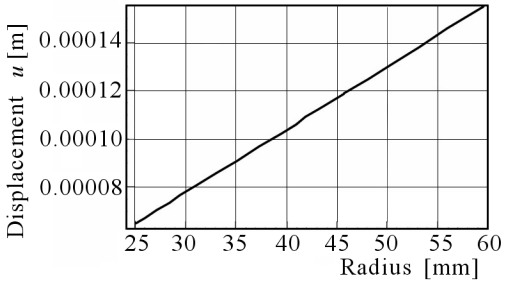


Fig. 12. The displacement $u$ in function of the average radius ($\beta = 12°$)

## 5. The experimental model

The goal of experimental testing was to choose a mathematical model that would constitute the closest approximation to the real model, for which the area of hysteretic loop is closest to the experimental area. In order to perform experimental tests, the model of the friction pair in the ring spring was designed and built (Fig. 13). The model was made of 45 steel, and the basic geometrical parameters of the friction pair were the following: $r_z = 77\,\text{mm}$, $r_w = 63\,\text{mm}$, $\beta = 12°$. The overall structural is shown in Figure 4. It was designed in such a manner so that its position in the machine gripping jaws during the loading process would not change (Fig. 13 – elements 6 and 7). For measuring displacements of the system, extensometers were used with a measurement base of 10 mm and a measurement nominal range $\pm 1.2\,\text{mm}$ (sub-range of the nominal range $\pm 0.24\,\text{mm}$), which were included in the standard machine equipment (Fig. 14 – elements 2 and 3).

The way of attaching extensometers 2 and 3 to elements 1, 2 and 3 (Fig. 13) is presented in Fig. 14. On elements 3 and 5 (Fig. 13), steady pins 6 and 7 were located in order to ensure a coaxial measurement base for second extensometer (Fig. 14) in relation to the symmetry axis of the inner and outer part of the

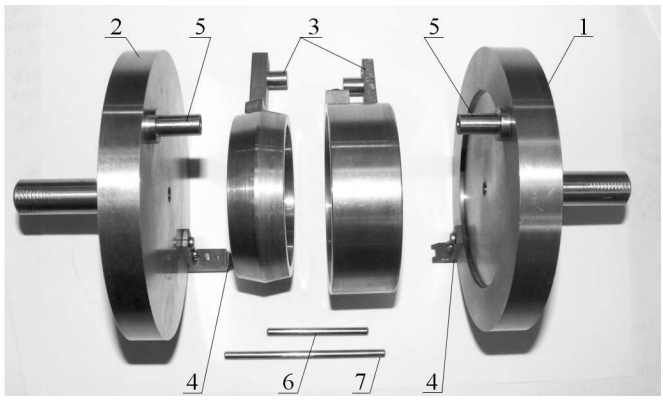


Fig. 13. Design of the experimental model of the friction pair of the ring spring (decomposed system): 1 – outer grip, 2 – inner grip, 3 – shears to position the coaxial friction pair and to fix an extensometer, 4 – grips to fix the second extensometer, 5 – shears to position the inner and outer grip, 6 – steady pin to position the friction pair, 7 – steady pin to position the inner and outer grip


Fig. 14. The mode of fixing the model and an overview of its components: 1 – tested model, 2 – first extensometer, 3 – second extensometer, 4 – gripping jaws of an MTS testing machine

friction joint (elements 1, 2 and 3 in Fig. 13). In order to provide the best conditions for cooperating joined elements (maximum contact surface, surface pressure, smoothness of motion), conical surfaces were subject to a surface treatment by very precise grinding.

## 6. Results of experimental tests

The tests were conducted on an MTS testing machine at the Institute of Machine Design Fundamentals of Warsaw University of Technology with the use of TestWareSX software. The mode of fixing the tested model is presented in Fig. 14. The methodology of the experiment consisted in loading the system up to the maximum value $P_{max}$ so that not to exceed a safe limit of material elasticity. Next, the system was unloaded down to the pre-assumed value $P_{min}$ and loaded up again. The loading process was controlled by a computer in such a way so that the torque moment would equal zero while the experiment was conducted. Before the measurement was started, both the extensometer and the control-measurement system were subject to calibration. A Mathematica 4.1 application was used to produce a graphical representation of the testing results (Fig. 15-Fig. 20). The programs enabled us, among other things, to calculate numerically the area of the hysteretic loop and to approximate the obtained graphs. A series of experiments was conducted, and selected results were shown in Fig. 15-Fig. 18. By modifying the loading parameters, we found singular (e.g. Fig. 18) and cyclic hysteretic loops (e.g. Figs. 15, 17, 18). Moreover, graphs were arranged to show the change of the loading force and the displacement of the joint in time (Figs. 16, 19). Figures 16 and 19 show characteristics $P(u)$, $P(t)$, $u(t)$ obtained for the model in four measurement cycles. In that case, the system was loaded up to $P_{max} = 20\,\text{kN}$ and $28\,\text{kN}$, and then unloaded down to $P_{min} = 1\,\text{kN}$. The whole process can be divided into four stages (Fig. 3).

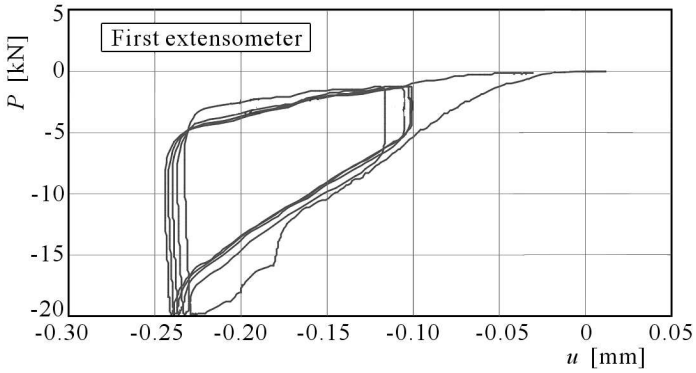


Fig. 15. An experimental hysteretic loop for the loading force $P_{max} = 20\,\text{kN}$, number of loading cycles: 4

The program enabled us to control the loading in the following manner: preliminary loading (increase of the force up to $P_{max}$ and maintaining the load for 10 s (for one or four loading cycles).

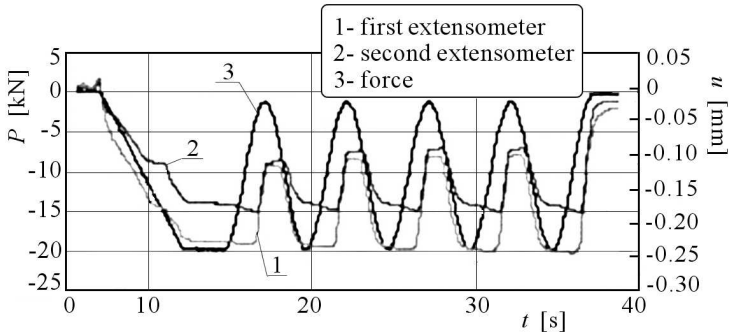


Fig. 16. Quadruple changes of the force and displacement in time for $P_{max} = 20\,\mathrm{kN}$

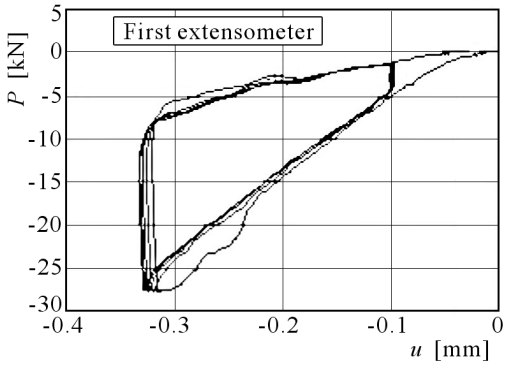


Fig. 17. An experimental hysteretic loop for the loading force $P_{max} = 28\,\mathrm{kN}$, number of loading cycles: 4

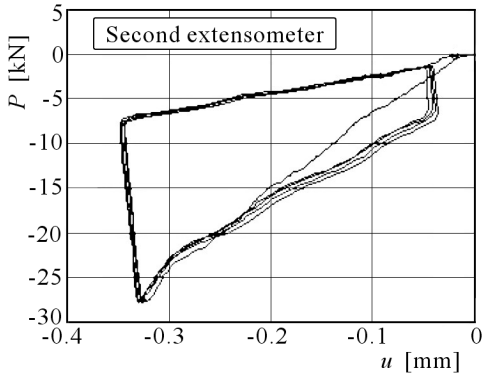


Fig. 18. An experimental hysteretic loop for the loading force $P_{max} = 28\,\mathrm{kN}$, number of loading cycles: 4

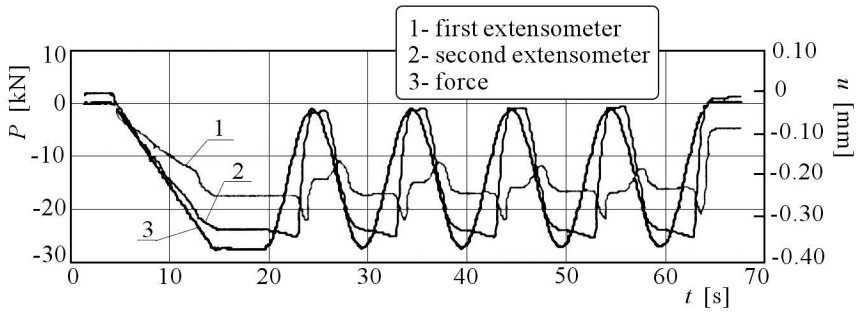


Fig. 19. Quadruple changes of the force and displacement in time of $P_{max} = 28\,\text{kN}$

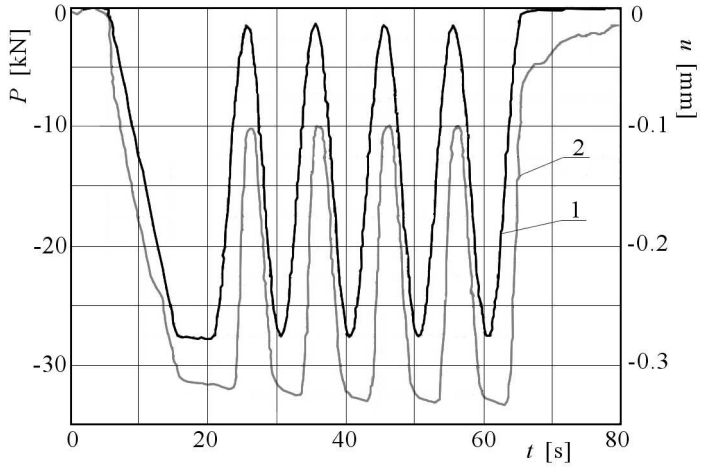


Fig. 20. Singular changes of the force (1) and displacement (2) in time

**Table 2.** Energy losses obtained from simulations and experimental tests

| No. | Load [KN] | Theoretical model $\psi$ [Nm] | Experimental model $\psi$ [Nm] |
|---|---|---|---|
| 1 | 15 | 0.000622 | 0.000685 |
| 2 | 20 | 0.001106 | 0.001159 |
| 3 | 28 | 0.002168 | 0.002224 |

To sum up, it should be noted that the separation of the phenomenon of structural friction in the experimental tests was very complicated and the obtained results were influenced by simplified assumptions and internal friction, which was neglected in theoretical considerations. In order to present the results of experiments in a graphical way, Microsoft Excel and Mathematica 4.1 programs were used. The programs enabled calculation of the area of hysteretic loops and to approximate the obtained graphs. Table 2 shows a

comparison of energy losses (the area of hysteretic loops) obtained as a result of simulations and experimental tests.

The value of dissipated energy is proportional to the area contained inside the hysteretic loop. The area was measured by a planimeter. The measurement of the system was calibrated. In order to achieve identical measures for the quantities, it was necessary to scale the measured systems and carry out necessary calculations.

The comparison was compiled for the joint of internal and external rings of the friction pair in the ring spring. Percentage differences between the results (areas of hysteretic loops) obtained numerically and experimentally are shown in Table 3.

**Table 3.** Differences (in %) between the average value (area of hysteretic loops) of the results obtained from experimental tests and numerical simulation

| No. | Loading [KN] | Difference [%] |
|---|---|---|
| 1 | 15 | 10.2 |
| 2 | 20 | 4.8 |
| 3 | 28 | 2.6 |

For better comparison, an average value of the hysteretic loop area obtained from experiments on the MTS testing machine was calculated.

## 7. Conclusions

The paper presents a mathematical model of a ring spring system and results of experimental tests on a real model conducted on an MTS testing machine. A comparative analysis allows one to formulate a conclusion that the pure friction model is more similar to the real one. Characteristics shown in Figures 15 and 17 are comparable – both quantitatively and quantitatively – in graphs showing the results of theoretical considerations (Fig. 13). The divergence between theoretical and experimental results is caused by simplifying assumptions made for the mathematical model. The following implifications contributed to the discrepancy: constant friction coefficient, neglected internal friction, unprecise construction of the real model, problems related to the fixing of the model in the testing machine (positioning in the gripping jaws) and difficulties occurring during measurements (elimination of clearances), problems with mounting of measurement elements.

## References


1. GIERGIEL J., 1990, *Tłumienie drgań mechanicznych*, PWN, Warszawa
2. GRUDZIŃSKI K., KOSTEK R., 2005, Influence of normal micro-vibrations in contact on sliding motion of solid body, *Journal of Theoretical and Applied Mechanics*, **43**, 37-49
3. KACZMAREK W., 2003, Analysis of a bolted joint with elastic and frictional effects occurring between its elements, *Machine Dynamics Problems*, **27**, 1, 21-40
4. KOSIOR A., SKUP Z., 2000, Badanie rozpraszania energii poprzez tarcie suche w połączeniu dwóch belek, *Proceedings of the International Conference "Friction 2000", Modeling and Simulation of the Friction Phenomena in the Physical and Technical Systems*, Warsaw University of Technology, 137-144
5. OSIŃSKI Z., 1998, *Damping of Vibrations*, A. A. BALKEMA, Rotterdam-Brookfield
6. SKUP Z., 1998, Wpływ tarcia konstrukcyjnego w wielotarczowym sprzęgle ciernym na drgania w układzie napędowym, *Prace naukowe, Mechanika*, **167**, Oficyna Wydawnicza PW
7. SKUP Z., KACZMAREK W., 2005, Badania teoretyczne i doświadczalne rozpraszania energii w połączeniu gwintowym z uwzględnieniem tarcia konstrukcyjnego, *XV konferencja nt "Metody i Środki Projektowania Wspomaganego Komputerowo"*, Politechnika Warszawska, 347-356


## Badania teoretyczne i doświadczalne rozpraszania energii dla modelu sprężyny pierścieniowej


Streszczenie

W pracy przedstawiono zagadnienie rozpraszania energii w modelu sprężyny pierścieniowej przy uwzględnieniu tarcia konstrukcyjnego. Przeprowadzono analizę porównawczą wyników teoretycznych uzyskanych metodą symulacji cyfrowej z wynikami badań eksperymentalnych przeprowadzonych na maszynie wytrzymałościowej MTS. W pracy omówione są rozważania teoretyczne, metoda przeprowadzenia badań oraz porównanie wyników badań.


*Manuscript received June 22, 2006; accepted for print December 20, 2006*